frontiers | Frontiers in Environmental Chemistry

ORIGINAL RESEARCH
published: 20 May 2022
doi: 10.3389/fenvc.2022.847682

Diamine-Appended Metal Oxide Framework Materials for Thermal-Swing Ad- and Desorption of Carbon Dioxide at Ambient Conditions

Kamal K. Maharjan, Philip B. Jørgensen*, Mohsen Rezaei and Matthew S. Johnson*

Department of Chemistry, University of Copenhagen, Copenhagen, Denmark

Carbon dioxide is a waste product of human metabolism that is unwanted in the indoor atmosphere. Here we test advanced materials that could be used to pump away carbon dioxide and thereby improve indoor air quality. Metal-organic framework (MOF) structures have a variety of properties that make them attractive for direct air capture (DAC) of CO_2. In this study, Mg_2 (dobpdc4- = 4,4-dioxidobiphenyl-3,3-dicarboxylate) and m-2-m-Mg_2(dobpdc) were evaluated for their ability to adsorb and desorb CO_2 at ambient atmospheric conditions via a thermal swing. The Mg_2(dobpdc) sample did not show appreciable interaction with CO_2 in contrast to the diamine-appended version. The molar occupancy of CO_2 on the active sites of m-2-m-Mg_2 (dobpdc) (m-2-m = N,N-dimethylethylenediamine) during adsorption and desorption was in the range of 5.6–11.8%. These experiments showed the rapid ad- and de-sorption of CO_2 by the MOF. Relative humidity was seen to be an important variable and the performance of the tested structures decreased slightly after several cycles of use.

Keywords: metal-organic framework, MOF, carbon dioxide, CO_2, environment, thermal swing, Mg_2(dobpdc), m-2-m-Mg_2(dobpdc)

OPEN ACCESS

Edited by:
Zhengyang Wang,
Connecticut Agricultural Experiment Station, United States

Reviewed by:
Jenny G. Vitillo,
University of Insubria, Italy
Peng Geng,
Frontage Laboratories Inc., United States

****Correspondence:***
Kamal K. Maharjan
kamalkubermaharjan@gmail.com
Philip B. Jørgensen
philip.becher@gmail.com

Specialty section:
This article was submitted to Sorption Technologies, a section of the journal Frontiers in Environmental Chemistry

Received: *03 January 2022*
Accepted: *19 April 2022*
Published: *20 May 2022*

Citation:
Maharjan KK, Jørgensen PB, Rezaei M and Johnson MS (2022) Diamine-Appended Metal Oxide Framework Materials for Thermal-Swing Ad- and Desorption of Carbon Dioxide at Ambient Conditions. Front. Environ. Chem. 3:847682. doi: 10.3389/fenvc.2022.847682

1 INTRODUCTION

Carbon dioxide in indoor environments is a concern due to its impacts on health including fatigue, impaired thinking, high blood pressure, unconsciousness and at very high levels, mortality (Azuma et al., 2018; Wis 2019; Du et al., 2020). In addition CO_2 is frequently used as a proxy for poor indoor air quality due to its association with bioeffluents including bioaerosol and other types of pollution. Dose-effect relationships for CO_2 have been established (Wis 2019). Mole fractions of 400–1,000 ppm are typical of indoor spaces with proper ventilation (Wis 2019).

There are a large number of methods for capturing CO_2 including scrubbers, bioconversion, precipitation or mineralization, adsorption, et. cetera, which are used in industry, only a few of them might be practicable in an indoor application. Reversible capture would appear to be the most manageable and practical technology for control of indoor CO_2. Several studies investigated the reduction of CO_2 in indoor environments via sorption-type air filters (Hu et al., 2016). Metal-organic frameworks (MOFs) are a new class of nanostructural adsorptive materials which have shown the capability of capturing various gas-phase compounds thanks to their ultra-high porosity and surface functionalization. It was found that MOFs are capable of selectively capturing CO_2 (Furukawa et al., 2010; Lu et al., 2010; Hu et al., 2019; Liu et al., 2016; Chen et al., 2017) reversibly, this advantage being in line with the goal of this study. As CO_2 can react with amines to form carbamate or bicarbonate

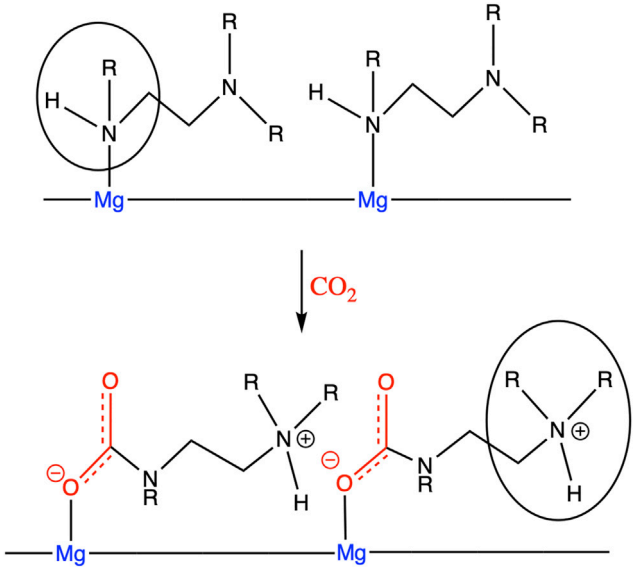

FIGURE 1 | This diagram is inspired from the work by Siegelman (Siegelman et al., 2017) and Martell (Martell et al., 2020) and shows the specific mechanism for the insertion of CO_2, resulting in ammonium carbamate chains.

ions, diamine-functionalized MOFs are very promising candidates for CO_2capture. There are many studies (McDonald et al., 2012; McDonald et al., 2015; Martell et al., 2020; Zhang et al., 2020a; Zhang et al., 2020b) that have been carried out show the capture CO_2 using diamine-appended dobpdc. There has been significant progress in designing new and better CO_2-capturing MOFs over the last decade. Mg_2-based structures are the most popular MOFs have been taken into consideration by researchers (McDonald et al., 2012; Yu and Balbuena, 2013; McDonald et al., 2015). For example, Zhang et al.'s findings state that a Mg_2-based MOF together with a Sc-based MOF showed the highest potential for CO_2 capture of the 11 metals used in their study (Zhang et al., 2020a). In this study two MOFs, one without amine functionalization, Mg_2 (dobpdc4- = 4,4-dioxidobiphenyl-3,3-dicarboxylate), and the other amended with an amine compound, m-2-m-Mg_2 (dobpdc) (m-2-m = N,N-dimethylethylenediamine), were used to capture CO_2.

Siegelman *et al* (Siegelman et al., 2017) examined mechanisms related to the interaction between CO_2 and diamine-appended MOFs. They found that these MOFs exhibit step-shaped CO_2 adsorption isotherms arising from CO_2 being inserted into the metal-amine bonds, creating ammonium carbamate chains. **Figure 1** shows the proposed mechanism for CO_2 insertion. A key point of the mechanism is that the diamine structure affects on the strength of both the Mg^{2+}amine bond and the ammonium carbamate interaction (Siegelman et al., 2017). The application of diamine-appended MOFs could prove to be useful in atmospheric conditions, by improving performance and delaying hydrolysis of the Mg-O bonds. In this work, the performance of the CO_2 adsorbants was studied in thermal swing mode under ambient atmospheric conditions. The goals of the study are to characterise the adsorbants by determining the amount of CO_2 they can adsorb, the change in performance over multiple adsorption/desorption cycles, the required temperature change, and the effect of humidity.

2 METHODS

2.1 Experimental Setup and Procedure

The MOF samples were synthesized using the method reported by Martell *et al.* (Long et al., 2018; Martell et al., 2020). A chamber made of Plexiglas was constructed (length, width and height: 0.52 m; volume: 0.14 m^3) to perform the tests. The chamber is shown in **Figure 2** schematically. A stainless-steel plate was used to support the MOF powders. First, the MOF was dissolved in methanol. The methanol-MOF mixture was put on the plate and left to evaporate, leaving a MOF-coated plate. The coated sample plate was weighed to determine the amount of MOF present in a sample. The sample plate was placed inside the chamber on a Peltier effect thermoelectric (TEC) cooler, which was placed over a heat-sink and exposed to the air inside the chamber. The chamber was sealed and the experiment was performed. A new MOF-coated plate sample was prepared for each experiment. The amount of m-2-m-Mg_2 (dobpdc) coated on the plate ranged between 0.220–0.423 g (5×10^{-4} to 1×10^{-3} mol).

The chamber had two walls made of metal and 4 contiguous walls made of plexiglass, for visibility. The front wall was detachable via screws with a rubber gasket to make an airtight seal.

As seen in **Figure 2**, ports allow access for wires and air sampling by a GaseraOne gas photoacoustic multi-gas analyzer. Inside the chamber, there were medium-sized fans (38 × 38 mm, flow rate = 31 m^3/h) connected to the floor and side-wall and a flow tube placed roughly in the middle of the chamber, which contained equipment as seen in **Figure 2**. Inside of the tower, there was a MOF-coated sample plate, a TEC plate (maximum voltage = 8.8 V), a heat-sink for the TEC plate, scaffolding to hold the heat-sink, and a fan underneath the tower (80 × 80 mm, flow rate = 52 m^3/h) for airflow to flow from beneath, into the tower.

The TEC plate was wired to an external DC power supply, which allowed for easy switching between heating and cooling. The maximum temperature reached was 78.3°C, whereas the minimum was 13.5°C.

2.1.1 Thermal Swing

This study uses thermal swing to test the conversion between adsorption and desorption of CO_2. Theoretically, as the specimen is cooled and heated up, it should adsorb and desorb CO_2 (Raganati et al., 2020). The temperature of the sample is controlled using Peltier effect controllers and measured using a thermocouple.

2.1.2 Measurements

The concentration of CO_2 in the chamber was measured using an online photo-acoustic sensor (GaseraOne), which also measures the other main greenhouse gases, CO_2, N_2O, CH_4, H_2O, with a sub-ppm detection limit. The GaseraOne was

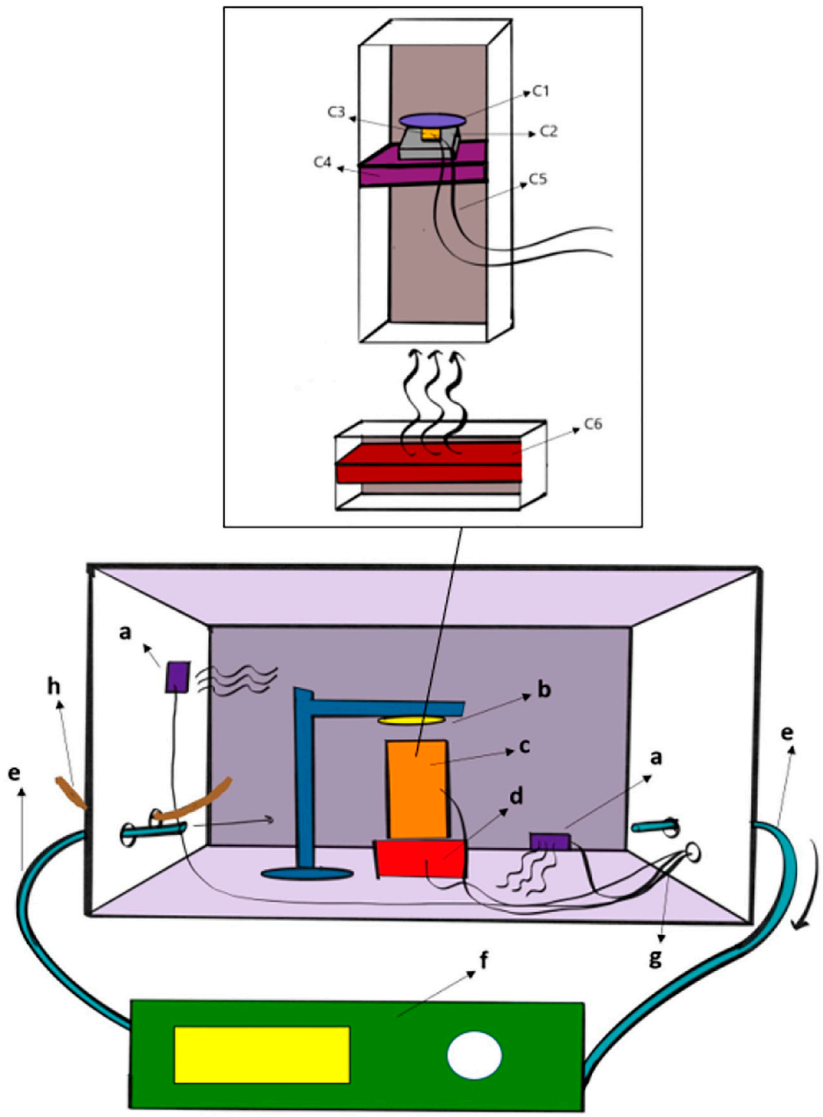

FIGURE 2 | Chamber layout; **(A)** Fans, **(B)** Infrared thermometer, **(C)** Funneling tower, **(D)** Air-permeable rack/fan, **(E)** Tubes for sampling in/out, **(F)** GaseraOne photoacoustic analyzer, **(G)** Wires, **(H)** Tube for adding CO_2, C1 - Sample plate, C2 - Heat sink, C3 - TEC plate, C4 - Scaffolding, C5 - Wires, C6 - Fan.

allowed to run until the CO_2 concentration reached a steady-state, to ensure equilibrium. Then, the sample was cooled to observe adsorption. Next the sample was heated leading to desorption of CO_2, allowing measurement of the capacity of adsorption during the next cooling period. This thermal swing was repeated, and the CO_2 concentrations were recorded by the GaseraOne. All tubes to measure the variables were connected to the chamber by Teflon tubes through different air-tight sampling ports.

A laser-thermometer (Fluke 64 MAX IR thermometer, with a basic accuracy of ±1°C) was suspended above the sample plate to measure the temperature of the MOF. There was a small tube on the left wall, shown in **Figure 2**, that was used to increase the CO_2 concentration artificially.

2.2 Calculations

Concentrations are measured using a GaseraOne photoacoustic trace gas monitor. Mole percent (mol%) is used in this work instead of weight percent (wt%), mmol/g, or cm^3/g (Lu et al., 2010; Liu et al., 2016; Chen et al., 2017) due to added chemical insight and ease in evaluating ad- or desorption of CO_2 relative to MOF active sites at the molecular level, as well as comparing to data for other MOFs.

Therefore, the mole fraction (mixing ratio) of $x(CO_2)$ in the gas phase was converted into amount concentration $c(CO_2)$ with the convention that negative values represent adsorption and positive, desorption. The amount concentration $c(CO_2)$ was multiplied by the volume of the chamber to yield the amount of CO_2 in the system.

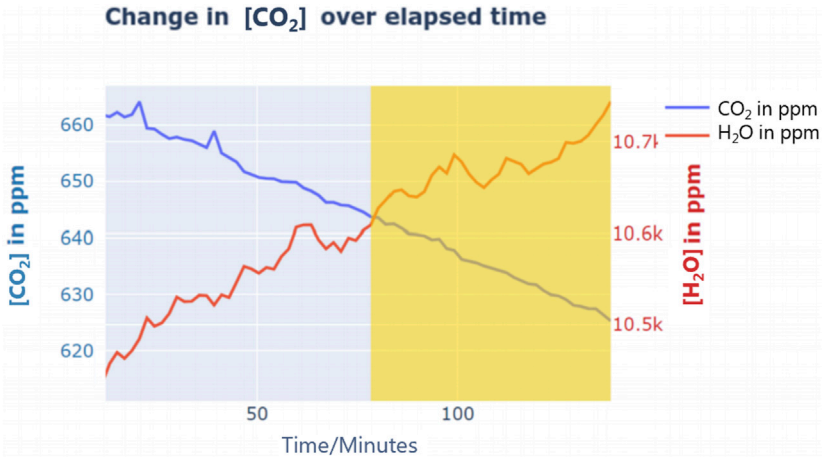

FIGURE 3 | A control experiment without any sample inside; the yellow region indicates when heating via the TEC plate occurred. Temperature swing between 13.5°C (adsorption) and 78.3°C (desorption).

The sample weight data were collected before and after coating the metal plate with m-2-m-Mg_2 (dobpdc). This difference was then converted from mass (g) to amount (moles). The molecular weight of $C_{18}H_{18}N_2O_6Mg_2$, i.e. m-2-m-Mg_2 (dobpdc), is 406.95 g/mol.

Finally, the occupation of CO_2 on MOF active sites was calculated using the amounts of adsorbed CO_2 and MOF active sites. A negative mole fraction represents desorption and positive, adsorption. The equation can be written as:

$$f = \frac{\Delta N\,(CO_2)}{N\,(MOF)} \tag{1}$$

where N is an amount in moles and f is a mole fraction of ad- or de-sorbed CO_2 relative to the number of MOF active sites.

3 RESULTS

Figure 3 shows a blank experiment performed without any sample in the chamber. This was essential to quantify the (small) background leak rate. The leak rate calculation is shown in **Eq. (2)**. The measurements of $x(CO_2)$ were taken at 20.5 and 80.3 min, thus Δt = 59.8 min, with a $\Delta x(CO_2)$ of 6.835 ppm.

$$r = \frac{\Delta x(CO_2)}{\Delta t} = \frac{6.835\,\text{ppm}}{59.8\text{min}} = 0.114\,\frac{\text{ppm}}{\text{min}} \tag{2}$$

This leak rate was incorporated into the experimental error as a limit on possible gas exchange, which is shown in **Table 1** as the error on the mass fractions and rates. Decay in other experimental trials could be explained also by combination of adsorption and leakage. The yellow-highlighted sections show the heating periods in each trial, whereas the blue periods between them represent cooling, i.e. desorption and adsorption, respectively. Each figure, from 3–9, shows x (CO_2) in ppm versus time, represented by the blue line. The plot of x (H_2O) vs. time shows the interaction of water with the material.

3.1 Mg_2(dobpdc)

Figure 4 shows the experimental results for Mg_2 (dobpdc). There is not a discernible difference between adsorption and desorption with respect to the thermal swing. This result was expected with this MOF as it has been also shown by Martell et al. (Martell et al., 2020).

3.2 m-2-m-Mg_2(dobpdc)

Figures 5–9 show the results of the effects of the thermal swing on the ambient concentration of CO_2. Overall, when the thermal swing was heating the plate, the concentration of ambient CO_2 increased due to desorption of CO_2 from the MOF. Conversely, when the plate was being cooled, the concentration of ambient CO_2 decreased due to adsorption of CO_2 onto the MOF. These changes in concentration are shown in **Tables 1** and **2**.

4 DISCUSSION

The major difference between this study and others, e.g. Hu Z. (Hu et al., 2019), Martell (Martell et al., 2020), Siegelman (Siegelman et al., 2017), etc., lies in the conditions at which these MOF substances were tested. In those studies experiments were conducted using thermal gravimetric analysis (TGA), which uses operational condition including pressure and temperature controlled as well as a pure inlet gas stream. In contrast the present study was performed under ambient conditions and feed gas flow. In TGA, one is able to continuously measure the amount of a species while changing temperature and gas composition. In contrast this experiment shows m-2-m-Mg_2 (dobpdc) is effective for use in thermal swing adsorption applications at ambient conditions. One of the main challenges in building practical devices is to find methods of retaining this good performance through multiple cycles of operation; in present form it degrades rapidly (Martell et al., 2020).

TABLE 1 | Mole % of CO_2 on MOF.

Date	1st Heating Cycle (%)	Time run (min)	Rate (%/min)	1st Cooling Cycle (%)	Time run (min)	Rate (%/min)
09/07/2020	−12.6 ± 2.4	24.3	−0.5 ± 0.1	6.4 ± 2.5	26.2	0.2 ± 0.1
10/07/2020	−12.1 ± 3.5	30.0	−0.4 ± 0.12	12.3 ± 6.0	52.3	0.2 ± 0.11
21/07/2020	−2.2 ± 1.2	18.7	−0.1 ± 0.06	7.0 ± 0.9	15.0	0.5 ± 0.06
17/08/2020	−32.9 ± 4.3	54.4	−0.5 ± 0.08	19.3 ± 2.6	31.8	0.6 ± 0.08
17/08/2020, overnight	−11.3 ± 2.8	37.5	−0.3 ± 0.08			
Average Mole % CO_2 on MOF(μ)	−14.2 ± 2.8			11.3 ± 3.0		
Standard deviation (σ)	10.1 ± 1.1			5.2 ± 1.8		
μ Rate (%/min)			−0.4 ± 0.09			0..4 ± 0.09
σ Rate(%/min)			0.2 ± 0.02			0..2 ± 0.02
Date	**2nd Heating Cycle (%)**	**Time run (min)**	**Rate (%/min)**	**2nd Cooling Cycle (%)**	**Time run (min)**	**Rate (%/min)**
09/07/2020	−5.8 ± 2.0	20.6	−0.3 ± 0.1	6.9 ± 4.6	48.6	0.1 ± 0.09
10/07/2020	−6.0 ± 3.5	29.9	−0.2 ± 0.12	8.3 ± 3.7	31.8	0.3 ± 0.12
21/07/2020						
17/08/2020*	−14.5* ±0.8	9.4*	−1.5* ±0.08	7.3* ±0.9	11.3*	0.6* ±0.08
17/08/2020, overnight						
Average Mole % CO_2 on MOF(μ)	−5.9 ± 2.8			7.6 ± 4.2		
Standard deviation (σ)	0.1 ± 0.8			0.7 ± 0.5		
μ Rate (%/min)			−0.2 ± 0.16			0.2 ± 0.11
σ Rate(%/min)			0.04 ± 0.01			0.1 ± 0.01

**values not included in calculations.*

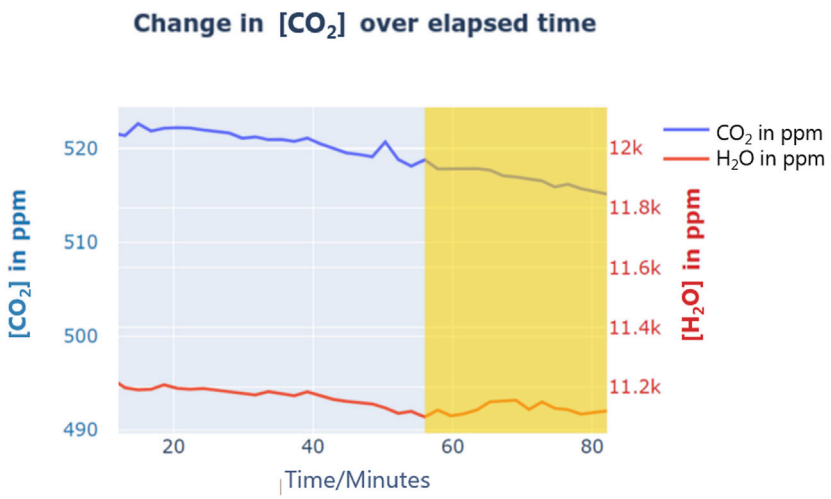

FIGURE 4 | Experiment with Mg_2 (dobpdc), i.e. non-diamine-doped MOF, where the yellow region shows when heating via the TEC plate occurred. Temperature swing was between 13.5°C (adsorption) and 78.3°C (desorption).

4.1 Mg_2(dobpdc)

Martell *et al.* conducted several experiments with Mg_2 (dobpdc), the non-appended version of our target compound and characterised CO_2 ad- and de-sorption kinetics for this compound (Martell et al., 2020). However, due to rapid degradation of the exposed Mg_2 sites to oxygen, water, and other oxidizing compounds as stated by Vitillo and Bordiga (Vitillo and Bordiga 2017), this non-diamine-appended version of the MOF was not suitable for testing CO_2 adsorption-desorption kinetics via thermal swing. The preparation method using methanol as stabilizing solvent before commencing the experiments might be a significant reason to cause Mg_2 (dobpdc) degradation, according to (Vitillo and Bordiga 2017).

In our tests of Mg_2 (dobpdc), there was no noticeable thermal-swing-induced activity. As seen in **Figure 4**, even though the thermal swing was activated, the level of CO_2 steadily decreased, without any notable desorption present. A possible reason can be due to an almost non-efficient cooling period adsorption of CO_2 by the un-appended MOF, and thus, nothing to be desorbed during the heating up period. This was expected based on isotherms measured on literature at RT (Vitillo and Ricchiardi, 2017). The steady decrease of humidity in the chamber can be linked to the strong water affinity of the considered MOF (Vitillo and Bordiga, 2017), which can slightly desorb the adsorbed water even when cooling, **Figure 4**. Therefore, this MOF showed no activity which may be due to hydrolysis of the unprotected active

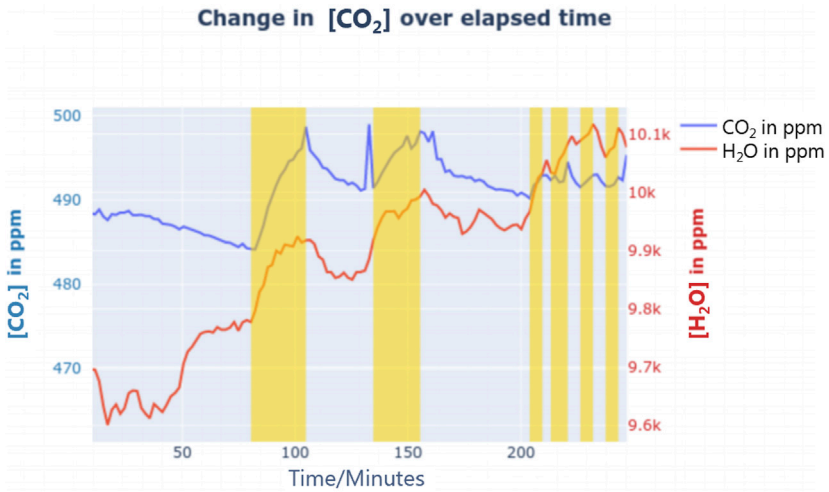

FIGURE 5 | A typical thermal swing experiment with m-2-m-Mg_2 (dobpdc), where the yellow regions show heating via the TEC plate occurring, and the clear regions showing the cooling periods. This experiment also has rapid-switching, which starts just after the 200 min. Temperature swing was between 13.5°C (adsorption) and 78.3°C (desorption).

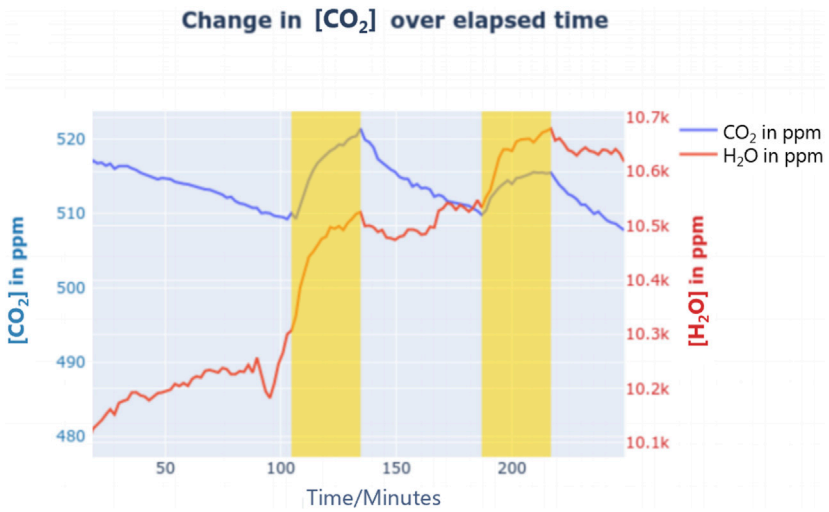

FIGURE 6 | A typical thermal swing experiment with m-2-m-Mg_2 (dobpdc), where the yellow regions show the heating periods via the TEC plate, and the clear regions after show the cooling periods. Temperature swing was between 13.5°C (adsorption) and 78.3°C (desorption).

sites on the Mg_2. In contrast, m-2-m-Mg_2 has diamine appendices that protect it from such damage, allowing for the enhanced adsorption of CO_2 at RT. We recommend that preventing this type of degradation is prioritised in future research.

4.2 m-2-m-Mg_2(dobpdc)

By appending Mg_2 (dobpdc) with diamines it is possible to achieve more selective CO_2 capture while minimizing the risk of oxidation via water, oxygen, nitric oxide, etc., effectively increasing the stability of the MOF (Vitillo and Bordiga 2017; Martell et al., 2020). In particular, we conducted experiments on m-2-m-Mg_2 (dobpdc), because of its superior stability to its non-diamine-doped analogue. This material showed more favorable properties for CO_2 capture as can be seen in **Figures 5–9**. A typical thermal swing experiment can be seen in the initial period of **Figure 5**. The end of the same figure shows a trial of rapid thermal cycling. Experiments of this kind were used to determine the CO_2 uptake parameters shown in **Table 2**. **Figure 5** shows the first successful experiment. For each period of heating (yellow-highlighted regions), we observed an increase in $x(CO_2)$, relating to desorption, and for each period of cooling (the transparent regions between the heating periods), we observed a decrease in $x(CO_2)$, relating to adsorption. For most of these experiments, we allowed the temperature to settle

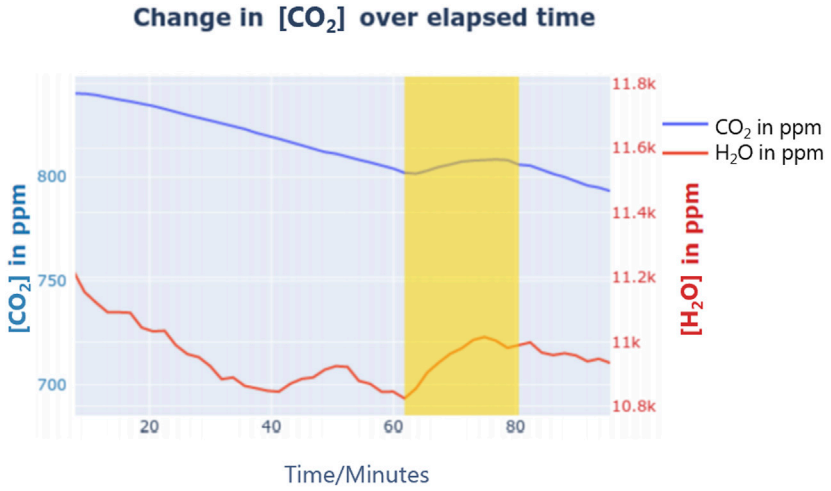

FIGURE 7 | A typical thermal swing experiment with m-2-m-Mg_2 (dobpdc), where the yellow region shows the heating period via the TEC plate, and the clear regions after shows the cooling period. Temperature swing was between 13.5°C (adsorption) and 78.3°C (desorption).

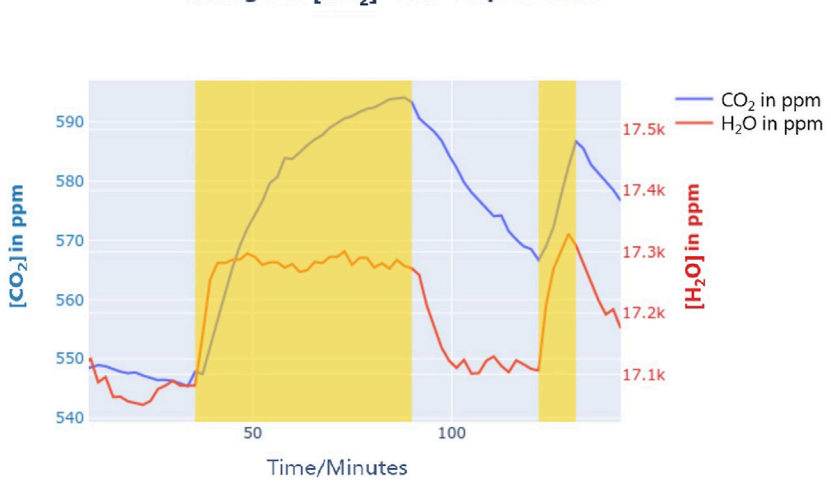

FIGURE 8 | A typical thermal swing experiment with m-2-m-Mg_2 (dobpdc), where the yellow regions show the heating periods via the TEC plate, and the clear regions after show the cooling periods. Temperature swing was between 13.5°C (adsorption) and 78.3°C (desorption).

over a lengthened period of time, between 0.5 and 1 h, however as shown in **Figure 5**, we observed that a series of fast-switches between heating and cooling resulted in noticeable capture kinetics. This demonstrates that these compounds are capable of working rapidly. The kinetics of CO_2 desorption and adsorption were already reported by MacDonald (McDonald et al., 2015) although for a higher partial pressure of CO_2.

Table 2 shows the calculated mole percentages from the fast-switching portions from **Figure 5**. For example, in the first cycle in **Figure 5**, we calculate the CO_2 mole fraction as (0.57 μM)/(4.5 μM) ≈ 0.126 = 12.6% per mole MOF. There were four heating periods and three cooling periods. Besides the outlier of the cycle 3 cooling (0.05% CO_2 on MOF) data-point, the other results showed gradual loss in capture capacity of the MOF, due to possible degradation via oxidation or morphological rearrangement. These rearrangements could be caused by switching between adsorptive and desorptive states, leading to the active sites being blocked over time.

4.3 Analysis of Thermal Swing Sorption

We gathered the results from these experiments and averaged them, in order to more accurately represent the capture capacity of the MOF.

The first heating cycle removed much of the CO_2 that was captured due to equilibrium with the air while preparing the sample. The average occupancy of CO_2 on the amine-MOF was

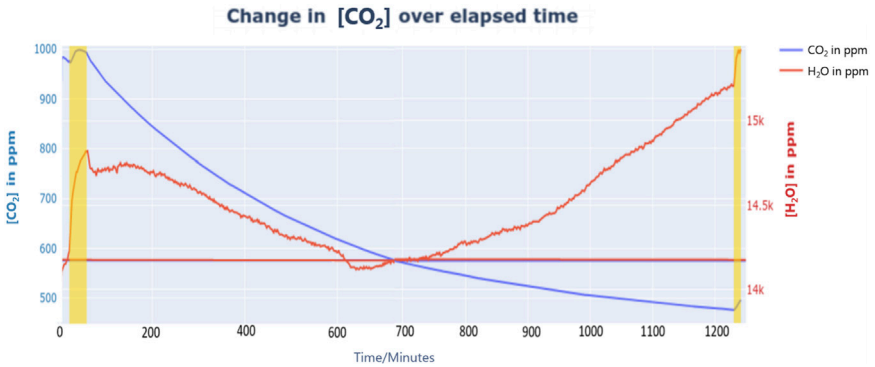

FIGURE 9 | A typical overnight thermal swing experiment with m-2-m-Mg_2 (dobpdc), where the yellow regions show the heating periods via the TEC plate, and the clear regions after show the cooling periods. This experiment shows a noticeable increase in gas concentrations after the second heating period, showing potential efficiency of m-2-m-Mg_2 (dobpdc) even after long-term exposure. Temperature swing was between 13.5°C (adsorption) and 78.3°C (desorption).

TABLE 2 | Mole % for Fast Switching of Thermoswing on 9 July 2020 Sample. All times were ≈5.6 min.

	Mole % CO_2 on MOF for Heating	Mole % CO_2 on MOF for Cooling
Cycle 3	-2.3 ± 0.6	0.05 ± 0.6
Cycle 4	-1.4 ± 0.6	2.6 ± 0.6
Cycle 5	-1.2 ± 0.6	1.1 ± 0.6
Cycle 6	-0.9 ± 0.6	-

0.57 micro mole (corresponding mole fraction about 14.2 ± 2.8% of carbon dioxide), meaning that this amount of CO_2 is desorbed per mole of MOF, with a standard deviation of 10.1 ± 1.1%.

The first cooling cycle in each experiment tested the capture capacity of the MOF. The average occupancy of CO_2 on MOF was 11.3 ± 3.0%, with a standard deviation of 5.2 ± 1.8%. The second heating cycles showed a lower average occupancy than the first, at −5.9 ± 2.8%, with a standard deviation of 0.1 ± 0.8%. The second cooling cycles showed a lower occupancy than the first, at 7.6 ± 4.2%, with a standard deviation of 0.7 ± 0.5%.

As is evident from the average occupancies as we transitioned between heating and cooling cycles, the capacity or depth of the material decreased with each cycle. The average occupancy is ~ |8|% lower from the first to the second (for heating), whereas the standard deviation has been lowered by ~ 9%. The first to second cooling shows a decrease in occupancy of ~ |4%|, and a change in standard deviation of ~ 4.5%.

4.3.1 Material Stability and Lifetime

The key feature in the effectiveness of MOFs for CO_2 capture is that they have a favorable pore size and affinity for CO_2. These properties can also limit the lifetime of the materials as they can decrease stability. The crystallinity of the MOF is altered when the CO_2 molecules are removed, due to capillary force-driven destruction (Mouchaham et al., 2018). A study by Zhao *et al.* showed structural dynamics of a MOF (ZIF-7) induced by CO_2 flow (Zhao et al., 2019). While this is not the same MOF as the one we tested (m-2-m-Mg_2 (dobpdc)), ours may display similar mechanisms, shown in **Figure 10**. This capillary force-driven destruction can lead to severe structural changes, therefore affecting the exposure and efficacy of the active sites on the MOF.

Another important cause of the gradual degradation of capacity in our MOF may be that there is a progressive oxidation of the MOF active sites by ambient O_2 and NO_2 which may be accelerated by the presence of H_2O (Vitillo and Bordiga 2017; Martell et al., 2020). H_2O and O_2 in particular are very abundant. We believe that further investigation of the morphological changes to the adsorbent material could help improving affinity, capacity, and selectivity towards CO_2 (Deng et al., 2020).

4.4 Rates of Adsorption and Desorption

Results for the rates of ad- and de-sorption are collected in **Table 1**. For the first heating and cooling cycles all data points were included in the analysis as none were more than 4σ from the mean. For the second cycle we omitted the starred data points due to their deviations from the mean. The fast-switching regions from **Figure 5** were analyzed separately into **Table 2**. During this experiment, the ad- and desorption of CO_2 onto MOF was still noticeable. This is an important example because it suggests that prolonged exposure is not necessary and might even be detrimental, due to the deterioration of the specimen.

4.5 Thermal Swing

The temperature range for our thermal swing experiments ranged from 13.5 to 78.5°C. In contrast, Siegelman et al. (2017), Vitillo and Bordiga (2017), and Martell et al. (2020) used temperatures as high as 120°C. Interestingly, Martell *et al.* state that maximum adsorption is reached at 70°C (Martell et al., 2020). In the present work a switch from adsorption to desorption is observed between 25 and 30°C . In the present work effective desorption of CO_2 is observed at temperatures just above ambient (between 25 and 30°C), while adsorption was achieved quickly at

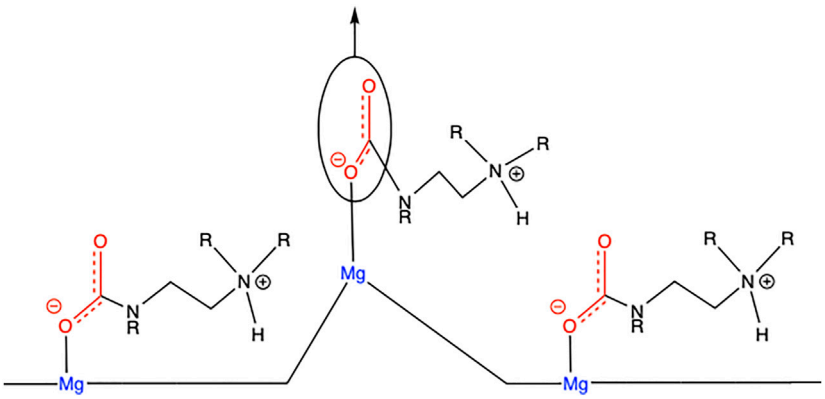

FIGURE 10 | Diagram of CO_2-induced capillary force-driven destruction of the MOF structure.

temperatures just below. We hypothesize that this is due to the change of matrix between their experiments and ours.

4.6 Effects of Humidity

As can be seen in **Figures 4–6**, the partial pressure of water vapor is much higher than that of carbon dioxide, and water is well known to be attracted to surfaces (Asay and Kim 2005). Our results show that water is likely to play an important role in modulating the interaction of CO_2 with the material. Similar effects were seen by Yu and Balbuena (2013) who tested a similar material and suggest that water blocks active sites. As seen in **Figure 3** there are not significant background fluctuations of water in the chamber. In contrast in **Figure 4**, while there is no CO_2 capture activity, there is a strong positive trend of H_2O, suggesting that H_2O is desorbed from the material on heating. We suggest that this desorption may play a role in deteriorating the activity of the material.

Figures 5–9 show concerted fluctuations of H_2O and CO_2, reinforcing the idea of water molecules competing with CO_2 for active sites (Erucar and Keskin 2020).

Water varies by over 300 ppm within a heating cycle and rapidly decays by over a 100 ppm upon cooling. One of the

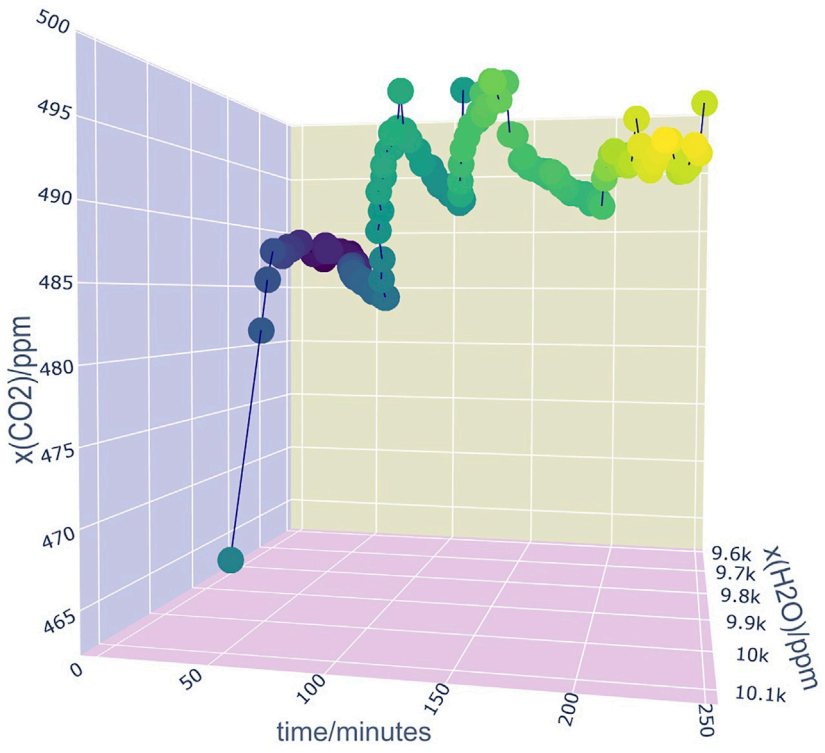

FIGURE 11 | 9 July 2020 3D Correlation plot between CO_2, H_2O, and time.

strongest examples is shown in **Figure 9**, because of the relatively large spike in [H_2O] during the final heating cycle, which was initiated after almost 20 h, suggesting that H_2O is captured in the MOF during the extended cooling period overnight. **Figure 11** shows a comparison of the correlation between CO_2 and H_2O concentrations from **Figure 5**. The dark colors of the curve represent lower values of [H_2O], whereas the lighter colors represent higher values. Thus, it is easy to see the correlation between CO_2 and H_2O adsorption and desorption activity. For viewing convenience, the 3D models are available online via the links presented here supplementary index 3D-graphs:

9/7/2020 (bit.ly/3i9yQWE)
10/7/2020 (bit.ly/2WoKRPC)
21/7/2020 (bit.ly/3xeFY8B)
17/8/2020 Ambient (bit.ly/3rGrywQ)

5 CONCLUSION

We have tested the ability of Mg_2 (dobpdc) and m-2-m-Mg_2 (dobpdc) under ambient atmospheric conditions for their ability to ad- and de-sorb CO_2 via thermal swing. We found that Mg_2 (dobpdc) showed no activity. We also saw that the sample degraded rapidly in ambient conditions presumably due to exposure to the atmosphere, potentially due to common, abundant atmospheric compounds such as O_2, H_2O, and NO_2. We conclude that the openly-accessible sites of Mg_2 (dobdpc) result in it not being suitable for ambient air CO_2 capture. In contrast m-2-m-Mg_2 (dobpdc) showed significant capture of CO_2.

Hydrolysis was slower in m-2-m-Mg_2 (dobpdc), we believe because of the diamine-appended Mg_2 sites, leading to a more robust material that better resists degradation. Our experiments showed that this material is successful in removing CO_2 from ambient air via thermal swing, but unfortunately performance still degrades over time. The m-2-m-Mg_2 (dobpdc) samples showed good capacity with occupancies of CO_2 on MOF reaching as high as 16.2% during cooling and −24.8% during heating.

Our experiments show that the material interacted with water vapor in a manner similar to CO_2 suggesting competition for active sites on the MOF. It would be interesting to test CO_2 sorption as a function of humidity swing, due to this synergistic behavior. Additional research on the effect of relative humidity in capture dynamics of CO_2 in ambient conditions via MOFs would be useful. We have shown that MOF compounds have the necessary capacity, but not yet the inertness necessary for use for direct air capture (DAC).

DATA AVAILABILITY STATEMENT

The raw data supporting the conclusions of this article will be made available by the authors, without undue reservation.

AUTHOR CONTRIBUTIONS

KM and PJ contributed equally to this work. MR and MJ helped design the experimental setup. KM and PJ performed all of the experiments, data analysis, and co-writing. KM, PJ, MR, and MJ reviewed and edited the manuscript. All authors read and approved the final manuscript.

FUNDING

This research was funded entirely by the Department of Chemistry at the University of Copenhagen and ACTRIS-DK.

ACKNOWLEDGMENTS

We would like to extend a special acknowledgement towards Jiwoong Lee from the University of Copenhagen for providing the MOF samples used during these experiments. We would also like to thank him for his input on proofreading, formatting and organizing the article.

REFERENCES

Asay, D. B., and Kim, S. H. (2005). Evolution of the Adsorbed Water Layer Structure on Silicon Oxide at Room Temperature. *J. Phys. Chem. B* 109, 16760–16763. doi:10.1021/jp053042o

Azuma, K., Kagi, N., Yanagi, U., and Osawa, H. (2018). Effects of Low-Level Inhalation Exposure to Carbon Dioxide in Indoor Environments: A Short Review on Human Health and Psychomotor Performance. *Environ. Int.* 121, 51–56. doi:10.1016/j.envint.2018.08.059

Chen, Y., Lv, D., Wu, J., Xiao, J., Xi, H., and Xia, Q. (2017). A New MOF–505@GO Composite with High Selectivity for CO_2/CH_4 and CO_2/N_2 Separation. *Chem. Eng. J.* 308, 1065–1072. doi:10.1016/j.cej.2016.09.138

Deng, J., Dai, Z., Hou, J., and Deng, L. (2020). Morphologically Tunable Mof Nanosheets in Mixed Matrix Membranes for Co2 Separation. *Chem. Mater.* 32, 4174–4184. doi:10.1021/acs.chemmater.0c00020

Du, B., Tandoc, M. C., Mack, M. L., and Siegel, J. A. (2020). Indoor CO_2 Concentrations and Cognitive Function: A Critical Review. *Indoor Air* 30, 1067–1082. doi:10.1111/ina.12706

Erucar, I., and Keskin, S. (2020). Unlocking the Effect of H_2O on CO_2 Separation Performance of Promising Mofs Using Atomically Detailed Simulations. *Industrial Eng. Chem. Res.* 59, 3141–3152. doi:10.1021/acs.iecr.9b05487

Furukawa, H., Ko, N., Go, Y. B., Aratani, N., Choi, S. B., Choi, E., et al. (2010). *Ultrah. porosity metal-organic Fram.* 329, 424–428. doi:10.1126/science.1192160

Hu, S.-C., Shiue, A., Chang, S.-M., Chang, Y.-T., Tseng, C.-H., Mao, C.-C., et al. (2016). Removal of Carbon Dioxide in the Indoor Environment with Sorption-type Air Filters. *Int. J. Low-Carbon Technol.* 12, 330–334. doi:10.1093/ijlct/ctw014

Hu, Z., Wang, Y., Shah, B. B., and Zhao, D. (2019). CO_2 Capture in Metal–Organic Framework Adsorbents: An Engineering Perspective. *Adv. Sustain. Syst.* 3, 1800080. doi:10.1002/adsu.201800080

Liu, X., Xiao, Z., Xu, J., Xu, W., Sang, P., Zhao, L., et al. (2016). A NbO-type Copper Metal–Organic Framework Decorated with Carboxylate Groups Exhibiting

Highly Selective CO_2 Adsorption and Separation of Organic Dyes. *J. Mat. Chem. A* 4, 13844–13851. doi:10.1039/C6TA02908F

Long, J. R., McDonald, T. M., and D'Alessandro, D. M. (2018). *Alkylamine Functionalized Metal-Organic Frameworks for Composite Gas Separations*.

Lu, C.-M., Liu, J., Xiao, K., and Harris, A. T. (2010). Microwave Enhanced Synthesis of MOF–5 and its CO_2 Capture Ability at Moderate Temperatures across Multiple Capture and Release Cycles. *Chem. Eng. J.* 156, 465–470. doi:10.1016/j.cej.2009.10.067

Martell, J. D., Milner, P. J., Siegelman, R. L., and Long, J. R. (2020). Kinetics of Cooperative CO_2 Adsorption in Diamine-Appended Variants of the Metal–Organic Framework Mg_2(dobpdc). *Chem. Sci.* 11, 6457–6471. doi:10.1039/D0SC01087A

McDonald, T. M., Lee, W. R., Mason, J. A., Wiers, B. M., Hong, C. S., and Long, J. R. (2012). Capture of Carbon Dioxide from Air and Flue Gas in the Alkylamine-Appended Metal–Organic Framework Mmen-Mg2 (Dobpdc). *J. Am. Chem. Soc.* 134, 7056–7065. doi:10.1021/ja300034j

McDonald, T. M., Mason, J. A., Kong, X., Bloch, E. D., Gygi, D., Dani, A., et al. (2015). Cooperative Insertion of Co 2 in Diamine-Appended Metal-Organic Frameworks. *Nature* 519, 303–308. doi:10.1038/nature14327

Mouchaham, G., Wang, S., and Serre, C. (2018). *The Stability of Metal–Organic Frameworks*. John Wiley & Sons. chap. 1. 1–28. doi:10.1002/9783527809097.ch1

Raganati, F., Chirone, R., and Ammendola, P. (2020). CO_2 Capture by Temperature Swing Adsorption: Working Capacity as Affected by Temperature and CO_2 Partial Pressure. *Industrial Eng. Chem. Res.* 59, 3593–3605. doi:10.1021/acs.iecr.9b04901

Siegelman, R. L., McDonald, T. M., Gonzalez, M. I., Martell, J. D., Milner, P. J., Mason, J. A., et al. (2017). Controlling Cooperative CO_2 Adsorption in Diamine-Appended Mg_2(dobpdc) Metal–Organic Frameworks. *J. Am. Chem. Soc.* 139, 10526–10538. doi:10.1021/jacs.7b05858PMID: 28669181

Vitillo, J. G., and Bordiga, S. (2017). Increasing the Stability of Mg_2(dobpdc) Metal–Organic Framework in Air through Solvent Removal. *Mat. Chem. Front.* 1, 444–448. doi:10.1039/C6QM00220J

Vitillo, J. G., and Ricchiardi, G. (2017). Effect of Pore Size, Solvation, and Defectivity on the Perturbation of Adsorbates in Mofs: The Paradigmatic Mg2 (Dobpdc) Case Study. *J. Phys. Chem. C* 121, 22762–22772. doi:10.1021/acs.jpcc.7b06252

Wis (2019). Carbon Dioxide Data Sheet. wisconsin department of health services. Available at: https://www.dhs.wisconsin.gov/chemical/carbondioxide.htm downloaded [Dataset] (Accessed nov 15, 2021).

Yu, J., and Balbuena, P. B. (2013). Water Effects on Postcombustion CO_2 Capture in Mg–MOF–74. *J. Phys. Chem. C* 117, 3383–3388. doi:10.1021/jp311118x

Zhang, H., Yang, L.-M., and Ganz, E. (2020a). Adsorption Properties and Microscopic Mechanism of Co2 Capture in 1, 1-dimethyl-1, 2-Ethylenediamine-Grafted Metal–Organic Frameworks. *ACS Appl. Mater. interfaces* 12, 18533–18540. doi:10.1021/acsami.0c01927

Zhang, H., Yang, L.-M., and Ganz, E. (2020b). Unveiling the Molecular Mechanism of Co2 Capture in N-Methylethylenediamine-Grafted M2 (Dobpdc). *ACS Sustain. Chem. Eng.* 8, 14616–14626. doi:10.1021/acssuschemeng.0c05951

Zhao, P., Fang, H., Mukhopadhyay, S., Li, A., Rudić, S., McPherson, I. J., et al. (2019). Structural Dynamics of a Metal–Organic Framework Induced by CO_2 Migration in its Non-uniform Porous Structure. *Nat. Commun.* 10, 999. doi:10.1038/s41467-019-08939-y

Conflict of Interest: MJ is co-founder of Airlabs a company which makes air filtration systems but not for CO_2.

The remaining authors declare that the research was conducted in the absence of any commercial or financial relationships that could be construed as a potential conflict of interest.

Publisher's Note: All claims expressed in this article are solely those of the authors and do not necessarily represent those of their affiliated organizations, or those of the publisher, the editors and the reviewers. Any product that may be evaluated in this article, or claim that may be made by its manufacturer, is not guaranteed or endorsed by the publisher.